



ORIGINAL RESEARCH

Open Access



# Predicting snag fall in an old-growth forest after fire

Kendall M. L. Becker<sup>1,2</sup> and James A. Lutz<sup>1,2\*</sup>

## Abstract

**Background** Snags, standing dead trees, are becoming more abundant in forests as tree mortality rates continue to increase due to fire, drought, and bark beetles. Snags provide habitat for birds and small mammals, and when they fall to the ground, the resulting logs provide additional wildlife habitat and affect nutrient cycling, fuel loads, and fire behavior. Predicting how long snags will remain standing after fire is essential for managing habitat, understanding chemical cycling in forests, and modeling forest succession and fuels. Few studies, however, have quantified how fire changes snag fall dynamics.

**Results** We compared post-fire fall rates of snags that existed pre-fire ( $n = 2013$ ) and snags created during or after the fire ( $n = 8222$ ), using 3 years of pre-fire and 5 years of post-fire data from an annually monitored, 25.6-ha spatially explicit plot in an old-growth *Abies concolor*–*Pinus lambertiana* forest in the Sierra Nevada, CA, USA. The plot burned at low to moderate severity in the Rim Fire of 2013. We used random forest models to (1) identify predictors of post-fire snag fall for pre-existing and new snags and (2) assess the influence of spatial neighborhood and local fire severity on snag fall after fire. Fall rates of pre-existing snags increased 3 years after fire. Five years after fire, pre-existing snags were twice as likely to fall as new snags. Pre-existing snags were most likely to persist 5 years after fire if they were  $> 50$  cm in diameter,  $> 20$  m tall, and charred on the bole to heights above 3.7 m. New snags were also more likely to persist 5 years after fire if they were  $> 20$  m tall. Spatial neighborhood (e.g., tree density) and local fire severity (e.g., fire-caused crown injury) within 15 m of each snag barely improved predictions of snag fall after fire.

**Conclusions** Land managers should expect fall rates of pre-existing snags to exceed fall rates of new snags within 5 years after fire, an important habitat consideration because pre-existing snags represent a wider range of size and decay classes.

**Keywords** *Abies concolor*, Low-severity fire, Moderate-severity fire, Old-growth forest, *Pinus lambertiana*, Rim Fire, Smithsonian ForestGEO, Snag fall, Snag persistence, Yosemite Forest Dynamics Plot

## Resumen

**Antecedentes** Los árboles muertos en pie (*snags* en idioma inglés), están siendo cada vez más abundantes en bosques a medida que la tasa de mortalidad se incrementa debido a incendios frecuentes, sequías, y a los escarabajos de la corteza. Los árboles muertos en pie (*snags* de ahora en más), proveen de hábitat para aves y pequeños mamíferos, y cuando caen sobre el suelo, los troncos resultantes proveen de hábitat adicional para la fauna, y afectan el ciclo de nutrientes, la carga de combustible y el comportamiento del fuego. Predecir cuánto tiempo los grandes troncos permanecerán en pie luego de un incendio es esencial para manejar el hábitat, entender el ciclo químico en

\*Correspondence:

James A. Lutz

james.a.lutz@gmail.com

Full list of author information is available at the end of the article



© The Author(s) 2023. **Open Access** This article is licensed under a Creative Commons Attribution 4.0 International License, which permits use, sharing, adaptation, distribution and reproduction in any medium or format, as long as you give appropriate credit to the original author(s) and the source, provide a link to the Creative Commons licence, and indicate if changes were made. The images or other third party material in this article are included in the article's Creative Commons licence, unless indicated otherwise in a credit line to the material. If material is not included in the article's Creative Commons licence and your intended use is not permitted by statutory regulation or exceeds the permitted use, you will need to obtain permission directly from the copyright holder. To view a copy of this licence, visit <http://creativecommons.org/licenses/by/4.0/>.

los bosques, y modelar la sucesión y los combustibles en los bosques. Pocos estudios, por supuesto, han cuantificado cómo el fuego cambia la dinámica de la caída de los *snags*.

**Resultados** Comparamos la tasa de caída post fuego de los *snags* que existían previo a un fuego en particular ( $n = 2.013$ ) con aquellos creados durante o posterior a ese fuego ( $n = 8.222$ ), usando datos de tres años previos al fuego y cinco años luego del fuego, monitoreados anualmente en una parcela espacialmente explícita de 26,5 ha en un bosque maduro mixto de *Abies concolor* y *Pinus lambertiana* en la Sierra Nevada de California, EEUU. La parcela se quemó a una severidad baja a moderada en el incendio de Rim de 2013. Usamos modelos forestales al azar para: 1) identificar predictores de caída de *snags* para aquellos *snags* preexistentes al fuego y para nuevos, y 2) determinar la influencia espacial de árboles vecinos y la severidad local, en la caída de *snags* luego del incendio. La tasa de caída de los *snags* preexistentes se incrementó tres años luego del incendio. Cinco años después del incendio, los *snags* preexistentes tenían el doble de chances de caer que los *snags* recientes debido al incendio. Los *snags* preexistentes tuvieron la posibilidad de permanecer en pie cinco años luego del evento de fuego si tenían  $> 50$  cm de diámetro,  $> 20$  m de altura, y estaban chamuscados en el tronco a alturas superiores a los 3,7 m. Los *snags* recientes post incendio pudieron persistir mejor si su altura era  $> 20$  m. La vecindad de otros árboles (i.e. su densidad) y la severidad local (i.e. daños a la corona causados por el incendio) dentro de los 15 m de cada *snag*, mejoraron levemente las predicciones de las caídas de los *snags* después del fuego.

**Conclusiones** Los manejadores de tierras deberían esperar tasas de caída más altas de los *snags* preexistentes dentro de los cinco años luego del incendio, que de los nuevos *snags* causados por el incendio. Esto debe tenerse en cuenta en la consideración del hábitat, ya que los *snags* preexistentes representan un rango más amplio de tamaños y clases de descomposición.

## Background

Snags—standing dead trees—and logs perform vital functions in forest ecosystems. Snags contribute to gradual chemical cycling while providing habitat for numerous species of birds and mammals (Thomas 1979; Raphael and White 1984; Harmon et al. 1986; Rabe et al. 1998; Meyer et al. 2005). When snags fragment or fall, the resulting logs provide denning habitat, protect movement pathways, and accelerate soil development by cycling carbon and nutrients at a faster rate than snags (Harmon et al. 1986; Bull and Heater 2000; Butts and McComb 2000; Ucitel et al. 2003; Cousins et al. 2015). Intersecting or stacked logs (sensu Lutz et al. 2021; their Figure 8) can spread fire, potentially killing vegetation and altering soil characteristics (Monsanto and Agee 2008; Knapp 2015). As tree mortality rates continue to increase in response to drought, bark beetles, and fire (van Mantgem et al. 2009; Allen et al. 2010), snags will become more abundant, and understanding post-fire snag dynamics will become more central to managing habitat and modeling fuels and fire behavior (Stephens et al. 2018, 2022; Goodwin et al. 2021).

Snag longevity depends on snag attributes, including bole and crown architecture, wood strength, and resistance to decay (Dunn and Bailey 2012). Large-diameter snags commonly persist longer than small-diameter snags (Morrison and Raphael 1993; Ritchie et al. 2013; Grayson et al. 2019), as do shorter snags, particularly those with broken tops (Dahms 1949; Morrison and

Raphael 1993; Everett et al. 1999; Chambers and Mast 2005; Russell et al. 2006; Battles et al. 2015; Grayson et al. 2019). Species differ in wood strength and susceptibility to decay. *Abies* snags typically persist longer than *Pinus* snags, potentially due to faster heartwood decay in *Abies* and higher bole breakage rates; in such cases, the standing portion of the snag persists longer because it is shorter and less susceptible to windthrow (Morrison and Raphael 1993; Russell et al. 2006; Das et al. 2016). In contrast, stems with root rot (e.g., *Heterobasidion annosum*, *Armillaria* spp.) are prone to structural weakness at the base, which may increase their chance of falling, even if the bole is not highly decayed (Harmon et al. 1986; Cousins et al. 2015).

Studies of snag longevity have previously focused on two snag populations, trees killed by fire (Grayson et al. 2019) and trees killed by other causes (Keen 1929; Mitchell and Preisler 1998; Conner et al. 2005; Garber et al. 2005; Russell and Weiskittel 2012; Runkle 2013; Battles et al. 2015; Ganey et al. 2021). Little is known, however, about snags that existed before a fire and remain standing after fire. The ecological importance of this pre-existing snag population is expanding as more forest burns each year (Parks and Abatzoglou 2020). Pre-existing snags may have recruited gradually, from different causes of death, and are likely to represent a range of size and decay classes, especially in old forests (Conner et al. 2005). When a stand-level mortality event results in a pulse of new snags, pre-existing snags can function

as lifeboats for species, meeting the size and decay class requirements that the new cohort of snags may not provide for years or decades (Franklin et al. 2000).

The attributes of pre-existing snags determine how species use them and how long they remain standing after fire. When the attributes of pre-existing snags differ from fire-killed snags, we expect snag fall rates to vary between these populations, but *how* fall rates would differ is unclear: pre-existing snags may include larger individuals that are less likely to burn through at the base but are more likely to fall due to advanced decay (Keen 1929; Garber et al. 2005; Russell and Weiskittel 2012); in contrast, fire-killed trees may be smaller and therefore fall sooner (Gaines et al. 1958; Innes et al. 2006; Grayson et al. 2019). Local fire behavior should also alter snag dynamics by consuming stems at the base and increasing resistance to decay through charring, but whether the sum of these effects increases or decreases snag longevity is unknown. As both pre-existing and fire-killed snags become more abundant in forests, an improved understanding of snag longevity after fire is needed to manage habitat and parameterize fuel models.

We monitored 39,026 spatially explicit stems before and after a low- to moderate-severity fire to compare annual fall rates of pre-existing snags and snags created in or after the fire. Specifically, we (1) identify important predictors of snag fall after fire for pre-existing and new snags and (2) determine if including spatial neighborhood or local fire severity improves predictions of snag fall. We expected higher local fire severity to increase consumption at the stem base, making it more likely for both pre-existing and new snags to fall after fire.

## Methods

### Study area

The Yosemite Forest Dynamics Plot (YFDP; 37.77° N, 119.92° W) is a 25.6-ha study area in an unlogged, old-growth *Abies concolor*–*Pinus lambertiana* forest in Yosemite National Park (Lutz 2015; Lutz et al. 2012; Fig. 1). Elevation within the YFDP ranges from 1774 to 1911 m. Between 1981 and 2010, the modeled mean daily low and mean daily high January temperatures were  $-0.5$  °C and  $9.7$  °C, respectively, and the mean daily low and high July temperatures were  $14.2$  °C and  $28.1$  °C, respectively; the mean annual precipitation was 1068 mm with the majority falling as snow (Prism Climate Group 2016). Principal tree species ordered by pre-fire live tree abundance include *Abies concolor* [Gord. & Glend.] Lindl. ex Hildebr. (white fir), *Pinus lambertiana* Douglas (sugar pine), *Cornus nuttallii* Audubon ex Torr. & A. Gray (Pacific dogwood), *Calocedrus decurrens* [Torr.] Florin (incense-cedar), and *Quercus kelloggii* Newberry (California black oak) (Table 1).

Vegetation communities in the Sierra Nevada are strongly influenced by the presence and absence of fire (van Wagtenonk et al. 2020). The historical (pre-European settlement) fire regime of the YFDP was characterized by low- to moderate-severity surface fires and a mean fire return interval of approximately 30 years (Barth et al. 2015), slightly longer than the mean values for other lower montane mixed-conifer forests in the central Sierra Nevada (Scholl and Taylor 2010). Although lightning-ignited spot fires have occurred within the YFDP over the past century, the area has been largely fire-excluded since the last widespread event in 1900 (Scholl and Taylor 2010; Barth et al. 2015), leading to high tree density (Lutz et al. 2012; Barth et al. 2015) and surface fuel accumulation (Gabrielson et al. 2012, Lutz et al. 2014, Cansler et al. 2019).

On September 1 and 2, 2013, the YFDP burned in a fire set by park managers to control the spread of the Rim Fire (Stavros et al. 2016; Furniss et al. 2020). Fire severity within the YFDP as inferred from Landsat-derived scenes was largely low and moderate (Blomdahl et al. 2019). Both severity and spatial pattern were consistent with other fires in Yosemite since the mid-1970s (van Wagtenonk and Lutz 2007). The fire reduced aboveground live shrub biomass from 3490 to 269 kg ha<sup>-1</sup> (Lutz et al. 2017a) and consumed 79% of the total surface fuel loading, which had an average value of 192.0 Mg ha<sup>-1</sup> before the fire (Cansler et al. 2019).

### Data collection

The YFDP was installed in 2009 and 2010 following the protocols of the Smithsonian Forest Global Observatory (ForestGEO; Davies et al. 2021). The 25.6-ha area (800 m × 320 m) was subdivided into 20 m × 20 m cells, and field crews surveyed the corners of each cell with total stations (Lutz et al. 2012). Trees  $\geq 1$  cm diameter at breast height (DBH) and snags  $\geq 10$  cm DBH were tagged and mapped relative to the surveyed corners; DBH and species of each tagged stem were recorded. Snag height was measured with laser rangefinders (Impulse Rangefinder model 200, Laser Tech, Centennial, CO, USA), top diameter and percent of stem still standing were estimated, and each snag was assigned to one of five decay classes (1, least decayed; 5, most decayed) (Maser and Trappe 1984).

In annual demographic surveys that began in 2011 (Lutz 2015), field technicians documented recruitment (i.e., trees that had newly attained  $\geq 1$  cm DBH), tree mortality, and tree and snag fall (i.e., stem uprooted or snapped below DBH). These records associated each tagged individual with an annual status of live tree, snag, or log. Field crews recorded the DBH, height, top diameter, and percent of stem still standing for each new mortality. Logs  $\geq 50$  cm in diameter and  $\geq 1$  m long were

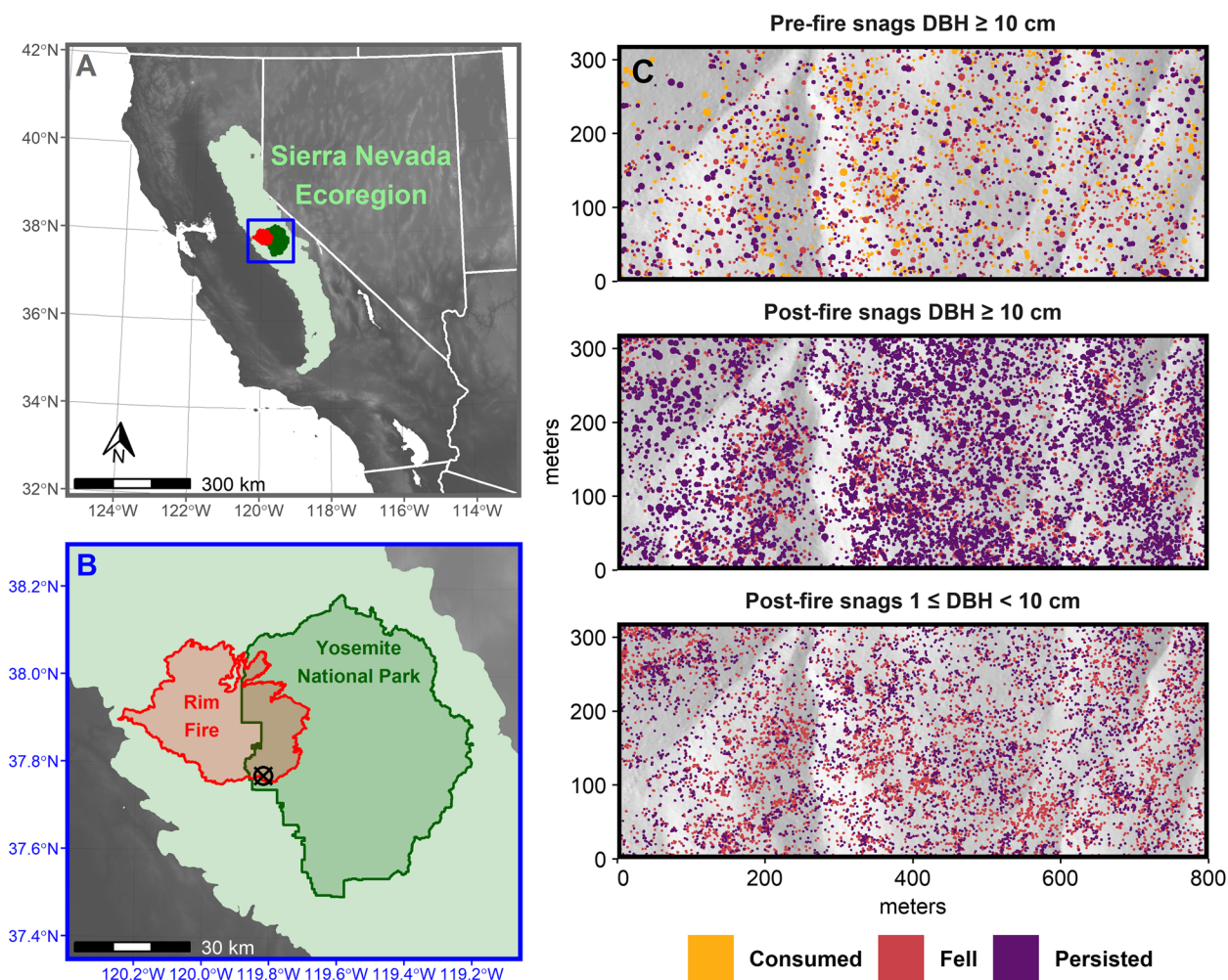


**Fig. 1** A, B The Yosemite Forest Dynamics Plot (YFDP) is a 25.6-ha permanent study area in an old-growth *Abies concolor*–*Pinus lambertiana* forest in Yosemite National Park in the central Sierra Nevada, CA, USA. The YFDP was installed in 2009 and 2010 and burned at low to moderate severity in the 2013 Rim Fire. Stem maps (C) show the snag outcomes in 2018 for snags that existed before the fire (pre-fire) and snags that were created in or after the fire (post-fire). Stem diameters appear four times larger than their measured size. Only the top panel includes consumed snags because trees that were consumed in the fire never became snags

mapped relative to stems and grid corners; length, short- and long-end diameters, and decay class were recorded.

In May 2014, following the Rim Fire, field crews reassessed the decay class and re-measured DBH, height, and top diameter of all snags documented before the fire. Stems were recorded as consumed if stem height was reduced to below DBH and no piece of bole  $\geq 1$  m long was found nearby. Percent crown injury was recorded for every tree that had been alive in 2013 (Varner et al. 2021). Maximum bole scorch height was recorded for all stems. Logs  $\geq 50$  cm in diameter and  $\geq 1$  m long were re-mapped and re-measured. If any piece of re-mapped log moved during the fire, this was noted. Unburned areas  $\geq 1$  m<sup>2</sup> were mapped relative to stems and grid corners (Blomdahl et al. 2019).

**Snag abundance, volume, biomass, and carbon content**

We used DBH, height, and top diameter measurements to calculate annual snag density, basal area, volume, biomass, and carbon (C) content by species, diameter class, and decay class for pre-fire and post-fire snag populations. We estimated snag volume as the sum of two conical frustums (i.e., decapitated cones), from the base of the stem to DBH and from DBH to the tip or break point of the bole. For conifers, we used species-specific equations from Wensel and Krumland (1983) to model the inside-of-bark diameter at the stem base and species-specific equations from Biging (1984) to model the inside-of-bark diameter at the top of the stem if the stem was broken. We used species-specific equations from Zeibig-Kichas et al. (2016) to

**Table 1** Abundance, density, and basal area of five species of snags in the Yosemite Forest Dynamics Plot. Pre-fire snags include snags inventoried at plot establishment in 2009 and 2010 and trees that died after plot establishment and before the fire in September 2013. Post-fire snags include trees that died in or up to 5 years after the fire (i.e., 2014–2018)

Snag population	Snag abundance	Density (snags ha <sup>-1</sup> )	Basal area (m <sup>2</sup> ha <sup>-1</sup> )
Pre-fire snags DBH ≥ 10 cm			
<i>Abies concolor</i>	1467	57.3	7.242
<i>Pinus lambertiana</i>	399	15.6	7.180
<i>Quercus kelloggii</i>	108	4.2	0.144
<i>Calocedrus decurrens</i>	36	1.4	0.465
<i>Cornus nuttallii</i>	3	0.1	0.002
Total	2013	78.6	15.033
Post-fire snags DBH ≥ 10 cm			
<i>Abies concolor</i>	6202	242.3	11.476
<i>Pinus lambertiana</i>	1162	45.4	11.462
<i>Quercus kelloggii</i>	387	15.1	0.502
<i>Calocedrus decurrens</i>	282	11	0.907
<i>Cornus nuttallii</i>	189	7.4	0.100
Total	8222	321.2	24.447
Post-fire snags 1 ≤ DBH < 10 cm			
<i>Abies concolor</i>	10,759	420.3	0.996
<i>Pinus lambertiana</i>	1777	69.4	0.143
<i>Quercus kelloggii</i>	1411	55.1	0.073
<i>Calocedrus decurrens</i>	601	23.5	0.053
<i>Cornus nuttallii</i>	232	9.1	0.020
Total	14,780	577.4	1.285

model bark thickness at DBH. If the stem was broken, we used species-specific equations from Wensel and Olson (1995) to model bark thickness at the base of the stem and at the top of the stem. For hardwoods, we used DBH to represent outside-of-bark basal diameter because allometric equations were not available for these species.

We estimated pre-fire and post-fire snag biomass by multiplying snag volume by species- and decay-class-specific density values from Cousins et al. (2015) or Harmon et al. (2008). Values from Cousins et al. (2015) were used whenever possible because they were based on wood samples from standing snags, whereas values from Harmon et al. (2008) were based on standing snags and logs combined. We estimated pre-fire and post-fire snag C content by multiplying snag biomass by species- and decay-class-specific C concentration values from Cousins et al. (2015). When specific

C concentration values were not available, we used 0.5 (Thomas and Martin 2012; Lutz et al. 2017b).

### Snag status transitions

We determined annual recruitment, persistence, fall, and consumption rates of snags by associating each stem with an annual transition status for 2011 through 2018: tree to snag, snag to snag, snag to log, or snag to consumed. We grouped snags as small ( $1 \leq \text{DBH} < 10$  cm), medium ( $10 \leq \text{DBH} < 60$  cm), or large ( $\text{DBH} \geq 60$  cm) and low decay (class 1), moderate decay (class 2), or advanced decay (class 3, 4, or 5). We chose these diameter classes to be consistent with other studies (Michel et al. 2014; Lutz et al. 2018; Furniss et al. 2020) and because snags < 10 cm DBH were not inventoried when the YFDP was established. For each snag diameter class, we calculated the probability of a stem undergoing each type of transition in each year (Additional file 1: Figs. S1–S11). Snags could transition between decay classes only in 2014, when the decay class was reassessed.

### Snag attributes

We characterized each snag by fixed, pre-fire, and post-fire attributes (Additional file 1: Table S6). Fixed snag attributes included species, years between fire and death (for just post-fire snags), and topography. Slope, aspect, topographic position, terrain ruggedness, and roughness were calculated in R using the terrain function in the raster package (Hijmans 2020). A 1-m digital elevation model was aggregated to 10 m × 10 m cells. Topographic metrics were calculated for each cell based on the cell and the surrounding eight 10 m × 10 m cells, and these values were assigned to the snags within the central cell. Pre-fire snag attributes included pre-fire DBH, height, and decay class. Post-fire snag attributes included post-fire DBH, height, decay class, bole scorch, crown injury (for just post-fire snags), and whether the snag was located in an unburned patch  $\geq 1 \text{ m}^2$  (Blomdahl et al. 2019).

### Neighborhood metrics

We used forest inventory data from 2013 to characterize the pre-fire spatial neighborhood around each snag in two ways. First, we calculated snag isolation, represented by the distance from each snag to the nearest tree, snag, or piece of log. We considered snag isolation because it is a less labor-intensive way to summarize neighborhood. Second, we calculated tree, snag, and log density metrics in five annuli with radii of 0–3, 3–6, 6–9, 9–12, and 12–15 m, expanding out from each snag (Additional file 1: Table S6). We considered five neighborhood sizes by including metrics from successive

annuli. Our purpose was to identify a threshold radius beyond which neighborhood no longer influences snag persistence after fire.

For annulus metrics based primarily on live trees (i.e., live tree density, density of new mortalities, density of newly fallen stems, and log density), we calculated density by five diameter classes. We defined these classes by identifying plot-wide DBH thresholds associated with an 80% (10 cm), 60% (15 cm), 40% (21 cm), and 20% (28 cm) 5-year mortality rate. We used DBH thresholds based on fire effects rather than arbitrary diameter classes so the neighborhood metrics would relate more directly to local fire severity, not just forest structure. For annulus metrics based on snags, we calculated the density of small, medium, and large snags (see the “[Snag status transitions](#)” section).

To characterize local fire severity around each snag, we calculated the same metrics using forest inventory data from 2014 and added metrics for consumed trees, snags, and logs (Table 2; Additional file 1: Table S6). Logs ( $\geq 50$  cm in diameter and  $\geq 1$  m long) that had been present before the fire were spatially adjusted back to their pre-fire location if they had moved. We determined log consumption by subtracting the post-fire volume and biomass from the pre-fire volume and biomass within each 1-m<sup>2</sup> area. We represented the influence of log consumption on snag fall by estimating the total fire radiative energy (FRE) reaching each focal snag from logs within 15 m that had been consumed (Additional file 1: Methods: Equation 1).

To represent the influence of neighborhood crown injury on snag fall, we developed equations using basal area and percent crown injury as a proxy for the volume of crown injured within each neighborhood annulus (Additional file 1: Methods: Equations 2–4). Lastly, we represented the influence of neighborhood bole scorch on snag fall by developing a metric where bole scorch of stems within 15 m of the focal snag was weighted by distance from the focal snag according to the inverse-square law (Additional file 1: Methods: Equation 5).

### Model framework

This study was designed to identify important predictors of snag fall for two snag populations, snags that existed before the fire (pre-fire snags) and snags that died in or after the fire (post-fire snags). For each snag population, the response variable was binary: 0 if the snag remained standing 5 years after the fire or 1 if the snag fell within 5 years after the fire. We created one set of models based on pre-fire predictors and another based on post-fire predictors (Table 2). Our purpose was to (1) produce results relevant to managers who only have access to pre-fire or post-fire data and (2) identify which fire effects most

improve snag fall predictions. For each set of models, we compared the predictive power of snag attributes, different types of neighborhood metrics, and different neighborhood sizes by running random forest models with unique subsets of predictors. We compared 14 models predicting the fall of pre-fire snags and 13 models predicting the fall of post-fire snags. Because neighborhood metrics extended to 15 m from each snag, only snags that were  $\geq 15$  m inside of the plot boundary were included as focal snags.

### Variable selection

For each model, we used the Boruta function (Kursa and Rudnicki 2010, 2020) to determine which variables were confirmed to influence snag fall (Additional file 1: Methods: variable selection—Boruta function variable confirmation). We removed variables that were not confirmed from future analyses.

Next, we selected and removed some remaining variables to avoid correlations among predictors at or above three thresholds,  $r = 0.7$ ,  $r = 0.5$ , and  $r = 0.3$  (Additional file 1: Table S7), because the importance values generated by random forest are not meaningful if the predictor variables are highly correlated (Additional file 1: Methods: variable selection—random forest variable importance function). We compared random forest models using predictor variables selected at these three thresholds to determine how sensitive our model results were to arbitrary thresholds (Additional file 1: Figs. S12, S13, and S14).

For each model, we selected predictors to remove by identifying all variables that correlated with other variables at or above the specified threshold (e.g.,  $r = 0.7$ ). We identified the pair of variables with the highest correlation. Then, we kept the variable in the pair that had higher correlations with other variables and removed all the variables it correlated with. This process was repeated until no pairs of variables correlated with each other at or above the specified threshold.

### Random forest models

We used the `randomForest` function (Cutler et al. 2007; Liaw and Wiener 2018) to determine which variables were important predictors of whether a snag fell within 5 years after the fire (1) or not (0). We computed model accuracy using 10-fold cross-validation. We calculated sensitivity (percent of outcomes correctly classified as fallen), specificity (percent of outcomes correctly classified as persisting), and PCC (percent of outcomes correctly classified, a weighted average of sensitivity and specificity). We repeated this procedure 15 times on each model using different seeds to ensure that our results were robust.

**Table 2** Descriptions of 14 sets of predictor variables for binary random forest models of snag fall after fire for pre-fire and newly dead post-fire snag populations. Each row represents a set of predictor variables. See Additional file 1: Table S6 for descriptions of the variables in each predictor variable category

Predictor set	Categories of predictors in each model													
	Snag attributes				Snag neighborhood metrics				Scale					
	Fixed	Pre-fire	Post-fire	Pre-fire isolation	Pre-fire annuli	Post-fire fixed	Post-fire isolation	Post-fire annuli	Neighborhood annuli (m)					
									0-3	3-6	6-9	9-12	12-15	
Post-fire	0-15 m	X		X				X		X	X	X		X
	0-12 m	X		X				X		X	X		X	
	0-9 m	X		X				X		X	X			
	0-6 m	X		X				X		X				
	0-3 m	X		X				X		X				
	Isolation	X		X										
Pre-fire	Attributes	X		X										
	0-15 m	X	X <sup>a</sup>							X	X	X	X	X
	0-12 m	X	X <sup>a</sup>							X	X	X		
	0-9 m	X	X <sup>a</sup>							X	X	X		
	0-6 m	X	X <sup>a</sup>							X	X	X		
	0-3 m	X	X <sup>a</sup>							X	X	X		
Isolation	X	X <sup>a</sup>										X		
Attributes	X	X <sup>ab</sup>												

<sup>a</sup> Models of the post-fire snag population did not include pre-fire snag attributes

<sup>b</sup> The model based just on fixed snag attributes was not included in the analysis

For each snag population (i.e., pre-fire snags or new post-fire snags) and predictor set (i.e., pre-fire or post-fire attributes and neighborhood metrics), we used the best performance in the lowest performing metric (e.g., specificity or sensitivity) to identify the most predictive collinearity threshold and the most predictive model within that group (Additional file 1: Figs. S12 and S13). We chose this method because there was little variation in PCC values among the models, and we wanted to identify the model that performed best at what the models in each group did worst (Additional file 1: Methods: random forest models).

For each of the selected models, we averaged variable importance values across runs with different seeds to determine the mean importance of each predictor variable. We report the five most important variables in each model (Tables 3 and 4) and include complete variable importance results in Additional file 1: Table S7.

### Partial dependence plots

For the models selected as “best,” we used the partialPlot function in the pdp package (Greenwell 2018) to visualize the relationships between snag fall and each of the nine most important, continuous predictor variables. We inspected the partial dependence plots and used values from the literature and natural breaks in the data to demarcate threshold values. We subset the snag fall data

**Table 3** The mean variable importance across 15 model runs for the five most important variables in the most predictive models of the post-fire fall of pre-fire snags  $\geq 10$  cm DBH

Predictor set	Snag population: pre-fire DBH $\geq 10$ cm	
	Variable	Mean importance
Post-fire	Model A: Neighborhood: 0–3 m; collinearity threshold: $r = 0.7$	
	<b>Post-fire DBH</b>	67.1
	<b>Post-fire snag height</b>	38.1
	<b>Bole scorch</b>	21.2
	Distance-weighted crown injury in 0–3 m circle	14.2
Pre-fire	Model B: Neighborhood: 0–15 m; collinearity threshold: $r = 0.7$	
	<b>Pre-fire DBH</b>	64.4
	<b>Pre-fire snag height</b>	27.5
	<b>Species</b>	10.8
	Pre-fire density of live trees $\geq 28$ cm DBH in 0–3 m circle	10.3
	Pre-fire basal area of live trees in 0–3 m circle	8.8

Snag attributes are in bold text. Neighborhood attributes are in plain text. Model letters correspond to Fig. 3

**Table 4** The mean variable importance across 15 model runs for the five most important variables in the most predictive models of the post-fire fall of newly dead post-fire snags  $\geq 10$  cm DBH

Predictor set	Snag population: post-fire DBH $\geq 10$ cm	
	Variable	Mean importance
Post-fire	Model C: Neighborhood: 0–6 m; collinearity threshold: $r = 0.7$	
	<b>Species</b>	61.5
	<b>Post-fire snag height</b>	55.7
	<b>Years between fire and death</b>	32.0
	<b>Bole scorch</b>	27.9
Pre-fire	Model D: Neighborhood: 0–3 m; collinearity threshold: $r = 0.5$	
	<b>Species</b>	81.6
	<b>Years between fire and death</b>	58.3
	<b>Topographic position</b>	46.6
	<b>Slope</b>	41.1
	<b>Aspect</b>	38.7

Snag attributes are in bold text. Model letters correspond to Fig. 3

according to these thresholds and ran the partialPlot function to depict interactions between snag fall and the three most important post-fire predictor variables. All analyses were conducted in R version 4.0.2 (R Core Team 2020).

## Results

### Fall rates of pre-fire snags

In 2009 and 2010, there were 2282 medium and 436 large snags, together representing 7.2% of total inventoried stems ( $n_{\text{stems}} = 37,546$ ; Fig. 2; Additional file 1: Tables S1–S3). During the pre-fire period from 2011 to 2013, recruitment rates ( $100 \times$  new snags/snags of the previous year) of medium and large snags ranged from 9.5 to 21.8% and exceeded fall rates ( $100 \times$  newly fallen snags/snags of previous year), which ranged from 0.0 to 4.4%. Pre-fire snags were more likely to persist through the fire year if they had a larger DBH and were less decayed. Snag fall rate in the fire year was highest for small snags (8.3%) and lower for medium (4.4%) and large (4.8%) snags.

The fire consumed 45.7% of small, 17.8% of medium, and no large pre-fire snags of low decay. Excluding the partial consumption of pre-fire snags that fell during the fire year, 51.3% of total pre-fire snag biomass was consumed; biomass of pre-fire snags of low decay was reduced by 39.1% for small, by 26.2% for medium, and by 25.3% for large snags (Additional file 1: Table S1).

Patterns of pre-fire snag fall during the post-fire period from 2014 to 2018 exceeded pre-fire fall rates and varied by diameter class and decay class (Fig. 2; Additional file 1: Tables S1–S3). Small snags had the highest fall rate of the three diameter classes 1 year after the fire (29.7%), and



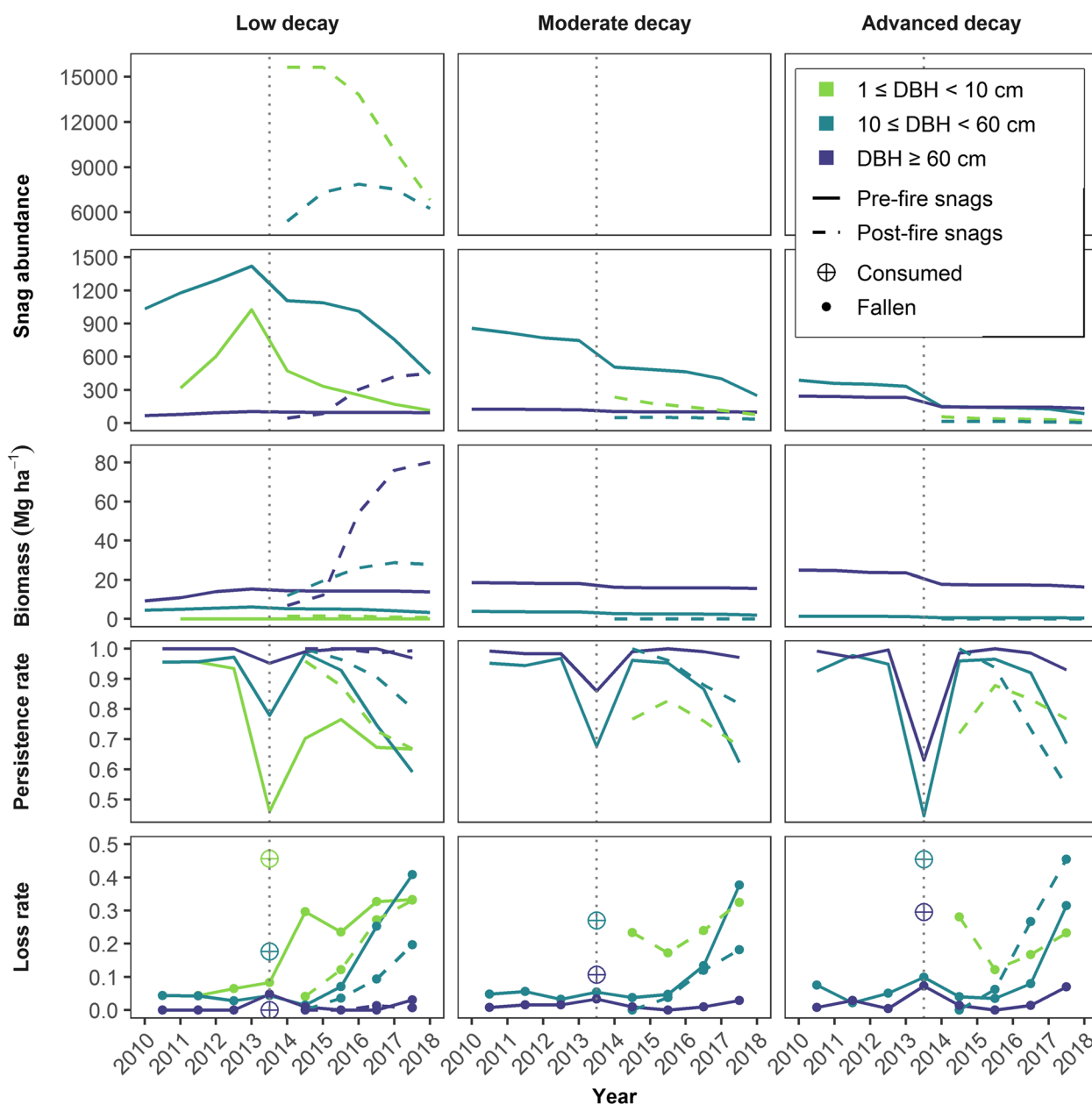


**Fig. 2** Snag dynamics in the Yosemite Forest Dynamics Plot from 2011 to 2018. Note the different y-axis scales for snag abundance. Snag persistence and loss rates were calculated as annual changes in the snag population between summer field seasons. The vertical dotted line represents the Rim Fire in the fall of 2013. In the fire year, snag loss is split into snag consumption and snag fall. All snags  $1 \leq \text{DBH} < 10$  cm died after 2010. Low decay: decay class 1; moderate decay: decay class 2; and advanced decay: decay class 3, 4, or 5

these rates remained high throughout the study period (23.5–33.3%), meaning that although the number of pre-fire snags still standing was reduced each year, a similar proportion of those snags fell annually. In contrast, the fall rate of medium snags decreased 1 year after the fire (1.5%) and then increased over the next 3 years, from 7.1 to 25.3 to 40.9%. As the number of medium pre-fire snags decreased during the post-fire period, a higher proportion

of those snags fell each year. Large snags of advanced decay were more likely to fall than less decayed snags, but this difference was not apparent until 4 years after the fire. Fall rates for large snags were low (0.0–2.3%) for the first 3 years after the fire. This changed in 2018, when 12.0–18.2% of large snags of advanced decay fell, compared with only 3.1% of large snags of low decay.

### Fall rates of post-fire snags

In the fire year, 15,925 small, 5472 medium, and 44 large snags were recruited, reflecting fire-year mortality rates of 77.6, 44.6, and 3.2% for the three size classes, respectively (Fig. 2; Additional file 1: Tables S4 and S5). The abundance of small snags remained high for 1 year after the fire and then decreased when fall rates (12.5–33.2%) far exceeded recruitment rates (0.5–0.7%). The abundance of medium snags increased for 2 years post-fire, then decreased, but biomass continued to increase through 2017, indicating that, within the medium-size class, smaller snags were falling as larger snags were recruited. Abundance of large snags increased substantially 3 years after the fire and represented 75.3% of the snag biomass in 2018.

### Snag fall model comparisons

For the four categories of random forest models (2 snag populations  $\times$  2 predictor sets), the most predictive models were associated with higher collinearity thresholds,  $r = 0.7$  and  $r = 0.5$  (Fig. 3). Among these selected models, the median PCC ranged from 68 to 75%. The median sensitivity (i.e., correctly classified fallen) and specificity (i.e., correctly classified persisting) ranged from 57 to 80% (Fig. 3). Random forest models of pre-fire snags were best at predicting snag fall, the more common outcome in that population, whereas models of post-fire snags were better at predicting snag persistence, the more common outcome in that population. When the post-fire snag dataset was balanced, models were better at predicting snag fall than snag persistence (Additional file 1: Fig. S14).

Models based on post-fire predictors had higher PCC by about 2% than models based on pre-fire predictors (Fig. 3). PCC increased by about 1% when any type of neighborhood predictor was included. When considering just the “best” model in each panel, no single neighborhood size was optimal. Neighborhood sizes of the “best” models ranged from a 3-m to a 15-m radius.

### Important predictors of snag fall

For pre-fire snags, DBH and snag height were the most important predictors of snag fall after fire (Table 3, Additional file 1: Table S7, Figs. S19 and S20). When pre-fire predictor variables were considered, species was the third most important variable, followed by two neighborhood metrics that represented the presence of medium and large trees within 3 m. Among post-fire predictors, bole scorch was the third most important predictor, followed by the neighborhood metric of crown injury to stems within 3 m; snag class was the fifth most important predictor.

For snags created in or after the fire, species and years between fire and tree death were important predictors of

snag fall (Table 4). When pre-fire variables were considered, size- and decay-class-related snag attributes were not included, and topographic position index, slope, and aspect were more important than pre-fire neighborhood variables (Additional file 1: Table S7). In models based on post-fire predictors, snag attributes were included, and snag height ranked just below species in importance. DBH was likely important as well but was removed prior to running the model due to a high correlation with height ( $r = 0.87$ , Additional file 1: Table S7). No neighborhood metrics were among the top five most important predictors for models of newly dead post-fire snags.

### Interactions of important variables

The fall rate of subpopulations of pre-fire snags ranged from 0.22 to 0.64 (Fig. 4). Fall rate was most sensitive to DBH. As DBH increased up to 50 cm, the fall rate decreased, then stabilized. Among larger snags ( $> 50$  cm DBH), higher bole scorch ( $\geq 3.7$  m) decreased the probability of falling. Taller snags ( $> 16$  m) were also less likely to fall.

Fall rate of subpopulations of post-fire snags  $\geq 10$  cm DBH ranged from 0.19 to 0.48 (Fig. 5). Fall rate decreased as post-fire snag height increased up to 20 m, at which point the fall rate stabilized. At all heights, the fall rate was higher for trees that died within 1 year of the fire and lower for trees that died 2 or more years after the fire. The fall rate was barely higher for *P. lambertiana* compared to *A. concolor*, and this difference was only observed among snags that died 2 or more years after the fire.

### Discussion

This study is the first to report fall rates of pre-fire snags before and after fire and to compare fall rates of pre-fire and newly dead post-fire snags. Fall rates of pre-fire snags increased after low- to moderate-severity fire. By 3 years after fire, pre-fire snags were more than twice as likely to fall as newly dead post-fire snags (Fig. 2). These results are consistent with current understanding of how snag size, decay class, and fire interact. For a given size class, pre-fire snags would be more decayed than newly dead snags, making pre-fire snags more likely to fall (Garber et al. 2005; Russell and Weiskittel 2012). Pre-fire snags are also more likely to be consumed at the base during a fire than fire-killed snags due to lower water content (Campbell et al. 2007) and absent, thinner, or loose bark. Managers should expect low- and moderate-severity fire to reduce populations of large, decayed snags through consumption and accelerated snag fall, decreasing post-fire habitat quality and increasing subsequent fuel loads (Lutz et al. 2020). Although the loss of pre-fire snags during and after fire may be dwarfed by recruitment from the delayed mortality of large trees (Additional file 1: Tables S1 and S4), the new snag recruits will require

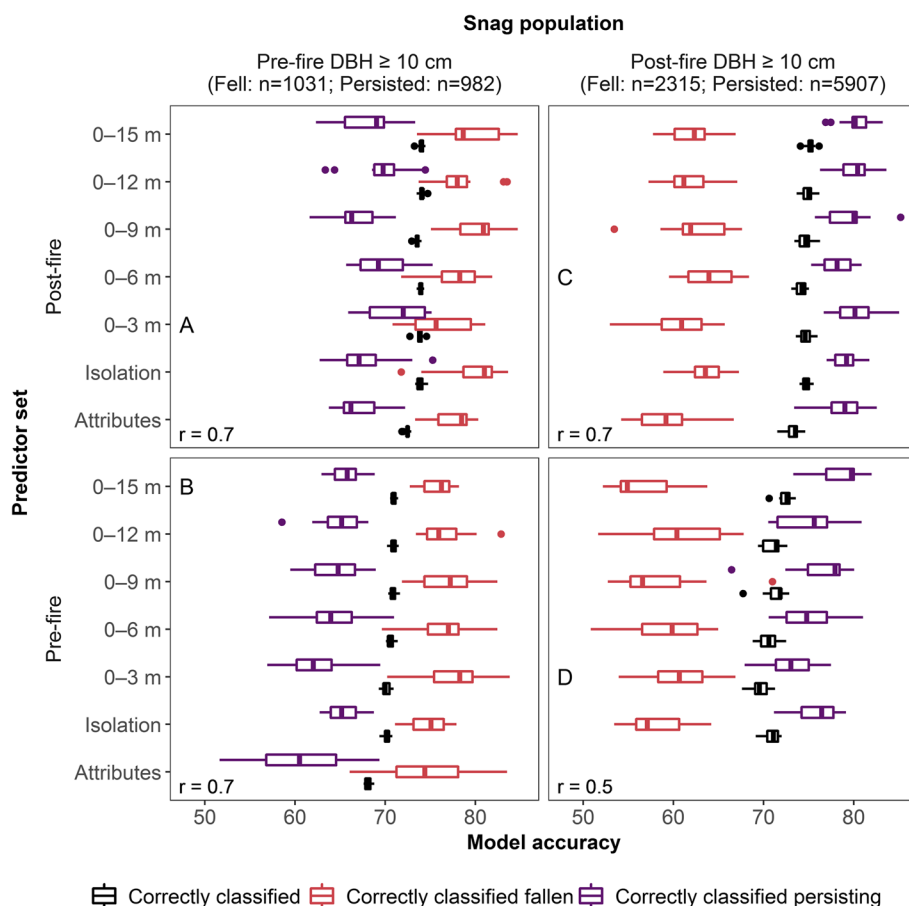


**Fig. 3** Accuracy metrics for the selected random forest models of snag fall within 5 years after fire for snags that existed before the fire (pre-fire) and snags that died in or after the fire (post-fire). Panel rows indicate whether the models were constrained to pre-fire or post-fire predictor variables. Within each panel, up to seven models occupy seven rows (see Table 2); the accuracy of each model is represented by the three boxplots that occupy that row. The boxplots represent the distribution of the model accuracy from 15 random forest analyses, each run with a different seed. **A–D** The models with the best performance in the lowest performing model accuracy metric for each snag population and predictor variable set. *r*-values in the lower-left corner of each panel indicate the collinearity threshold used to select the predictor variables in that panel (see the “Random forest models” section)

time to reach the moderate and advanced decay classes that characterize preferred vertebrate habitat (Thomas 1979; Raphael and White 1984). Longer-term studies are needed to determine how the different fall rates of pre-existing and newly dead post-fire snags affect the availability of snags of different size and decay classes through time.

**Snag attributes**

Previous research has shown that snag attributes, topography, and neighborhood metrics can improve predictions of snag fall (Everett et al. 1999; Chambers and Mast 2005; Russell et al. 2006; Grayson et al. 2019). Our models found that predictor variables in these categories were important, but the order of importance differed between pre-fire and newly dead post-fire snags. Snag attributes—such as species, DBH, height,

decay class, and bole scorch height—were better predictors of snag fall than topography, pre-fire spatial neighborhood, and local fire severity.

Species was moderately important for pre-fire snags but was the most important predictor for newly dead post-fire snags (Tables 3 and 4). For post-fire snags that died 2–4 years after the fire, fall rates tended to be slightly higher for *P. lambertiana* than *A. concolor* (Fig. 5). This result is consistent with previous research showing that *Pinus* spp. fall sooner than *Abies* spp. (Morrison and Raphael 1993; Dunn and Bailey 2012; Ritchie et al. 2013) and a species-specific comparison by Grayson et al. (2019) showing that *P. lambertiana* fell sooner than *A. concolor* during the first 10 years after death. The small difference in fall rates between *P. lambertiana* and *A. concolor* that we observed is also supported by a species-specific result from Bagne et al. (2008), who found that *P.*

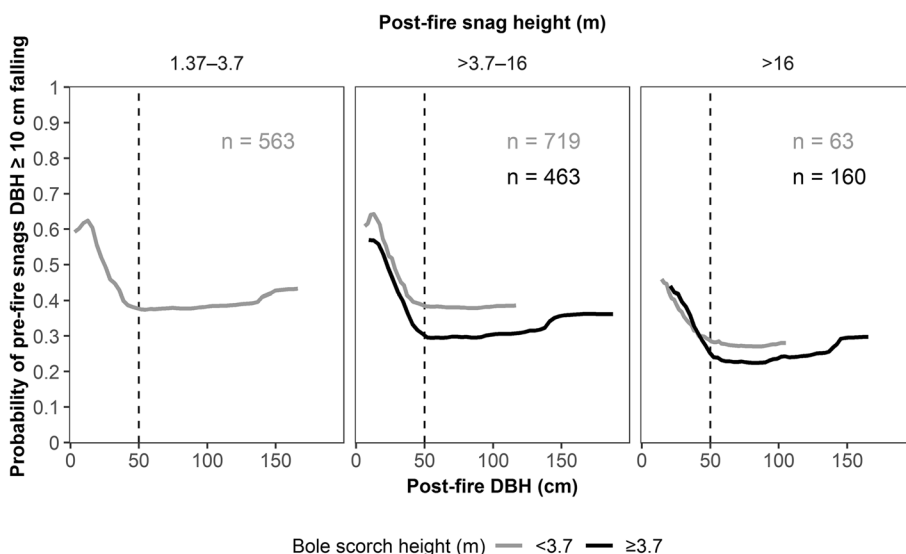


**Fig. 4** Multivariate partial dependence plots for the best model (Fig. 3A) that used post-fire variables to predict the fall of pre-fire snags  $\geq 10$  cm DBH. Data were subset based on important variables for that model: pre-fire snag height and bole scorch. Threshold values for pre-fire snag height were based on bird use snag height thresholds (Raphael and White 1984, their Table 11) (Additional file 1: Fig. S20). Threshold values for bole scorch were based on where the individual partial dependence plot for bole scorch passed from snags being more likely to fall to being more likely to persist (Additional file 1: Fig. S20). Black and gray lines represent the mean partial dependence values from 15 model runs. The dashed line at DBH = 50 cm indicates where fall rates start to plateau

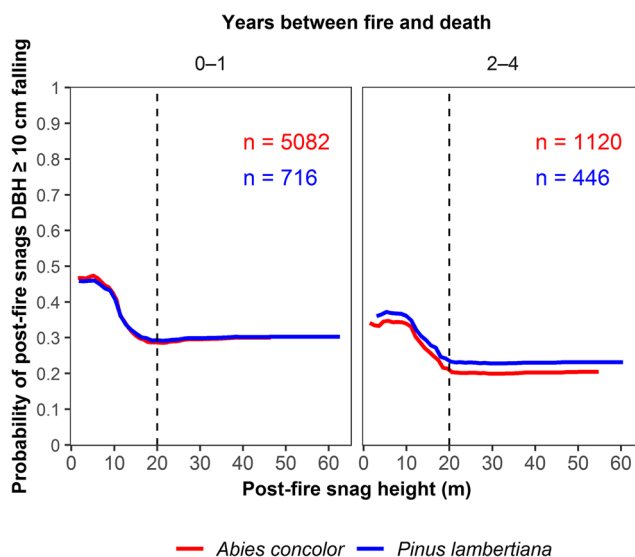


**Fig. 5** Multivariate partial dependence plots for the best model (Fig. 3C) that used just post-fire variables to predict the fall of post-fire snags  $\geq 10$  cm DBH. Data were subset based on important variables for that model: species and years between fire and tree death. Lines represent the mean partial dependence values from 15 model runs. The dashed line at height = 20 m indicates where fall rates start to plateau

*lambertiana* and *A. concolor* snags were equally likely to fall 1 year after prescribed fire.

For pre-fire snags, DBH supplanted species as the most important predictor variable (Fig. 4). Fall rates for pre-fire snags dropped sharply as DBH increased to 50 cm, but beyond this DBH threshold, fall rates stabilized at lower values (i.e., 0.2–0.4). Because our study took

place in an old-growth forest with a substantial population of large-diameter trees, the 50-cm DBH threshold at which fall rates stabilized is meaningful: 392 pre-fire snags (19.5%) had a pre-fire DBH  $\geq 50$  cm, and 326 pre-fire snags (16.2%) had a post-fire DBH  $\geq 50$  cm. The low fall rates for pre-fire snags  $> 50$  cm DBH support work by Grayson et al. (2019), who found that post-fire

snags  $\geq 50$  cm DBH were likely to persist for 10 years after death.

Numerous studies of post-fire snags have found that fall rate decreases with larger DBH (Dahms 1949; Lyon 1977; Morrison and Raphael 1993; Everett et al. 1999; Chambers and Mast 2005; Russell et al. 2006; Dunn and Bailey 2012; Ritchie et al. 2013; Battles et al. 2015; Grayson et al. 2019). This was clearly supported in our study as well, with only 28.2% of medium and large post-fire snags falling compared to 59.5% of small post-fire snags (Fig. 2). In fact, the difference in fall rates between the small size class and the larger size classes was greater than the difference between post-fire and pre-fire snags of the same size class—only 51.2% of medium and large pre-fire snags fell within the 5-year study period. Despite the obvious influence of DBH on the fall rates of post-fire snags, DBH was not included as a predictor in the final models because it was highly correlated with post-fire snag height (Additional file 1: Table S7).

Snag height was an important predictor for pre-fire and newly dead post-fire snags (Figs. 4 and 5). For both populations, fall rates decreased as height increased, until fall rate stabilized at lower values (i.e., 0.4) for snags taller than 20 m (Additional file 1: Figs. S19, S20, and S22). These results differ from several studies that found shorter snags were less likely to fall (Dahms 1949; Morrison and Raphael 1993; Chambers and Mast 2005; Russell et al. 2006). In the case of Dahms (1949) and Morrison and Raphael (1993), this difference could be attributed to the 11- to 15-year period between when the fire occurred and when snag monitoring began. However, Chambers and Mast (2005) and Russell et al. (2006) conducted studies within a similar time frame to ours. Another explanation could be the different species studied (only Morrison and Raphael [1993] included *A. concolor*) and the apparent tendency of the species in our study to break below 1.37 m (Grayson et al. 2019). Grayson et al. (2019) included both *A. concolor* and *P. lambertiana* and, similar to our result, found that taller snags were less likely to fall 10 years after death.

Years between fire and death was an important predictor of snag fall for newly dead post-fire snags. Trees that survived 2 or more years after fire had a lower chance of falling within 5 years of the fire (Fig. 5). This result is explained by the higher mortality rates for larger-diameter trees 3 and 4 years after the fire (Jeronimo et al. 2020); these snags would have been less likely to fall because of their larger DBH and lower degree of decay. However, our results differ from Grayson et al. (2019), who show that years between fire and death did not affect snag persistence for *A. concolor* and *P. lambertiana*. We attribute this inconsistency to the different time scales of our studies. Our analysis was limited to 5 years post-fire, so snags

that died 3 years after the fire only had 2 years in which to fall, whereas Grayson et al. (2019) monitored snags for 10 years after death.

Bole scorch height was an important predictor of snag fall for pre-fire and post-fire snags. Fall rates were generally lower for pre-fire snags with bole scorch  $\geq 3.7$  m tall, if DBH was  $> 50$  cm (Fig. 4). For post-fire snags, the fall rate decreased slightly as bole scorch increased to the height of 7 m (Additional file 1: Fig. S22). We had anticipated that fire might accelerate snag fall by consuming snags at the base but might also increase snag persistence if charred wood slowed colonization by decay fungi. Our data, however, did not support these mechanisms. The greater persistence of snags with higher bole scorch suggested that fire intensity at the snag base was not the primary factor controlling snag fall rates. Instead, we found that higher bole scorch correlated with post-fire snag height ( $r = 0.52$  for pre-fire snags and  $r = 0.41$  for post-fire snags; Additional file 1: Figs. S15 and S17) and consequently DBH and that the relationship to DBH was likely driving the perceived relationship between bole scorch height and snag fall. For example, among pre-fire snags with post-fire height from 3.7 to 16 m, those with bole scorch  $< 3.7$  m had a mean post-fire DBH of 19.0 cm, and 66.5% of them fell; those with bole scorch  $\geq 3.7$  m had a mean post-fire DBH of 39.8 cm, and just 39.3% of them fell. Mean post-fire snag height was similar between the two bole scorch groups (7.7 m and 8.1 m), indicating that bole scorch was more closely related to DBH than snag height. Given that post-fire DBH was the strongest predictor of snag fall for pre-fire snags (Table 3) and that higher bole scorch was a proxy for larger DBH, we suggest that larger DBH was more important to snag persistence than the effects of charring on the colonization rates of decay fungi.

Topographic variables were more important for predicting the fall of post-fire snags than pre-fire snags, but the magnitude of the effect was low (Table 4, Additional file 1: Table S7). For post-fire snags, fall rates were slightly higher on convex terrain, perhaps due to increased wind exposure (Additional file 1: Figs. S21 and S22). These results differ from a study by Everett et al. (1999), which found that snags were less likely to fall on convex terrain. Few other studies have found relationships between topographic variables and snag fall. Russell et al. (2006) considered slope and aspect as potential predictors of snag fall, but neither variable was included in the best models. Similarly, Dunn and Bailey (2012) found no relationship between slope or aspect and snag fall.

#### Neighborhood variables

Neighborhood metrics barely improved predictions of snag fall, similar to other studies that have found no

relationship between neighborhood and snag fall (Dunn and Bailey 2012; Ritchie et al. 2013; Grayson et al. 2019). We had expected higher local fire severity to increase fall rates due to greater consumption at the snag base. Instead, we found that charring from bole scorch made snags less likely to fall, likely due to a correlation with DBH, and that including neighborhood metrics only improved model PCCs by 1% (Figs. 3 and 4). Although the magnitude of the effect was low, pre-fire snags were slightly less likely to fall (< 8% change) if medium or large live trees were present within 3 m (Table 3, Additional file 1: Fig. S19), consistent with results from Chambers and Mast (2005) and Russell et al. (2006). The presence of larger neighbors might extend snag longevity by protecting the focal snag from windthrow. Our prevailing message, however, is that the relationship between neighborhood and snag fall was weak. We assessed the importance of neighborhood more directly than any prior study because we used spatially explicit measurements—not remote sensing (Russell et al. 2006), stand-level treatments (Ritchie et al. 2013), or non-spatially explicit stand metrics (Chambers and Mast 2005; Dunn and Bailey 2012; Grayson et al. 2019). The trivial 1% improvement in PCC associated with neighborhood predictors makes clear that managers should focus on species, diameter, height, bole scorch height, and decay class rather than neighborhood if the goal is to predict snag fall.

#### Study limitations and future directions

This study quantified the effects of fire on pre-fire snags and explored the relationship between local fire behavior and snag dynamics after fire. The scope of inference, however, was constrained by the low to moderate fire severity, the single forest type, and the single location. Recent studies show that abundant snags from prior fire, drought, and bark beetle mortality can fuel higher-severity fires and even mass fire behavior (Stephens et al. 2018, 2022; Goodwin et al. 2021). We would expect greater consumption of pre-fire snags from these events than we observed in our study area; still, snags with larger DBH would be the most likely to persist. Future studies should examine how pre-fire snags in different forest types are affected by a range of fire severities.

#### Conclusions

Predicting how long snags will remain standing after fire is important for managing habitat, understanding chemical cycling in forests, and modeling forest succession and fuels. In our study, pre-fire snags were at least twice as likely to fall as new snags within 3–5 years after fire. For pre-existing snags, diameter, height, and bole scorch height were better predictors of snag fall after fire than spatial neighborhood or local fire severity metrics.

Pre-existing snags were most likely to persist 5 years after a fire if they were > 50 cm in diameter, > 20 m tall, and charred on the bole above 3.7 m. When anticipating habitat availability and fuels, managers should expect fall rates of pre-existing snags to initially exceed fall rates of new snags.

#### Supplementary Information

The online version contains supplementary material available at <https://doi.org/10.1186/s42408-023-00225-z>.

**Additional file 1: Table S1.** Annual abundance, recruitment, and loss of pre-fire snags in the 25.6-ha Yosemite Forest Dynamics Plot. The Rim Fire burned the plot in the fall of 2013. Counts of snag recruitment and loss represent changes between the year of the row they are in and the next year. Only snags DBH  $\geq$  10 cm were inventoried at plot establishment. Beginning in 2011, mortalities of snags DBH  $\geq$  1 cm were documented. Snag diameter and decay class were remeasured in 2014. Recruitment and loss due to change represent snags that had reduced in size or entered a different decay class. Stems were recorded as consumed if stem height was reduced to below 1.37 m and no piece of bole  $\geq$  1 m long that belonged to that stem was found nearby. Snags that died in the fire year were considered post-fire snags. Biomass consumed does not include the partial consumption of pre-fire snags that fell during the fire. **Table S2.** Annual basal area and volume of pre-fire snags in the 25.6-ha Yosemite Forest Dynamics Plot. The Rim Fire burned the plot in the fall of 2013. **Table S3.** Annual biomass and carbon content of pre-fire snags in the 25.6-ha Yosemite Forest Dynamics Plot. The Rim Fire burned the plot in the fall of 2013. **Table S4.** Annual abundance, recruitment, and loss of post-fire snags in the 25.6-ha Yosemite Forest Dynamics Plot. The Rim Fire burned the plot in the fall of 2013. Counts of snag recruitment and loss represent changes between the year of the row they are in and the next year. Dynamics of pre-fire snags are reported in SI Tables 1–3. **Table S5.** Annual basal area, volume, biomass, and carbon (C) content of post-fire snags in the 25.6-ha Yosemite Forest Dynamics Plot. The Rim Fire burned the plot in the fall of 2013. Decay class 5 values were < 0.1 for every metric and are not reported. Dynamics of pre-fire snags are reported in Tables S1–S3. **Fig. S1.** Snag dynamics in the Yosemite Forest Dynamics Plot from 2011 to 2018 by density, basal area, volume, and carbon (C) content. The vertical dotted line represents the fire event in the fall of 2013. Because snags  $1 \leq$  DBH < 10 cm were not included in the dataset at plot establishment, all snags  $1 \leq$  DBH < 10 cm are trees that died after 2010. Low Decay: decay class 1; Moderate Decay: decay classes 2 or 3; Advanced Decay: decay classes 4 or 5. **Fig. S2.** Snag dynamics for *Abies concolor* (white fir) in the Yosemite Forest Dynamics Plot from 2011 to 2018. Snag persistence and fall rates were calculated as changes in the snag population between summer field seasons. The vertical dotted line represents the fire event in the fall of 2013. Because snags  $1 \leq$  DBH < 10 cm were not included in the dataset at plot establishment, all snags  $1 \leq$  DBH < 10 cm are trees that died after 2010. Low Decay: decay class 1; Moderate Decay: decay classes 2 or 3; Advanced Decay: decay classes 4 or 5. **Fig. S3.** Snag dynamics for *Abies concolor* in the Yosemite Forest Dynamics Plot from 2011 to 2018 by density, basal area, volume, and carbon (C) content. The vertical dotted line represents the fire event in the fall of 2013. Because snags  $1 \leq$  DBH < 10 cm were not included in the dataset at plot establishment, all snags  $1 \leq$  DBH < 10 cm are trees that died after 2010. Low Decay: decay class 1; Moderate Decay: decay classes 2 or 3; Advanced Decay: decay classes 4 or 5. **Fig. S4.** Snag dynamics for *Calocedrus decurrens* (incense-cedar) in the Yosemite Forest Dynamics Plot from 2011 to 2018. Snag persistence and fall rates were calculated as changes in the snag population between summer field seasons. The vertical dotted line represents the fire event in the fall of 2013. Because snags  $1 \leq$  DBH < 10 cm were not included in the dataset at plot establishment, all snags  $1 \leq$  DBH < 10 cm are trees that died after 2010. Low Decay: decay class 1; Moderate Decay: decay classes 2 or 3; Advanced Decay: decay classes 4 or 5. **Fig. S5.** Snag dynamics for *Calocedrus decurrens* in the Yosemite Forest Dynamics Plot from 2011 to 2018 by

density, basal area, volume, and carbon (C) content. The vertical dotted line represents the fire event in the fall of 2013. Because snags  $1 \leq \text{DBH} < 10$  cm were not included in the dataset at plot establishment, all snags  $1 \leq \text{DBH} < 10$  cm are trees that died after 2010. Low Decay: decay class 1; Moderate Decay: decay classes 2 or 3; Advanced Decay: decay classes 4 or 5. **Fig. S6.** Snag dynamics for *Cornus nuttallii* (Pacific dogwood) in the Yosemite Forest Dynamics Plot from 2011 to 2018. Snag persistence and fall rates were calculated as changes in the snag population between summer field seasons. The vertical dotted line represents the fire event in the fall of 2013. Because snags  $1 \leq \text{DBH} < 10$  cm were not included in the dataset at plot establishment, all snags  $1 \leq \text{DBH} < 10$  cm are trees that died after 2010. Low Decay: decay class 1; Moderate Decay: decay classes 2 or 3; Advanced Decay: decay classes 4 or 5. **Fig. S7.** Snag dynamics for *Cornus nuttallii* in the Yosemite Forest Dynamics Plot from 2011 to 2018 by density, basal area, volume, and carbon (C) content. The vertical dotted line represents the fire event in the fall of 2013. Because snags  $1 \leq \text{DBH} < 10$  cm were not included in the dataset at plot establishment, all snags  $1 \leq \text{DBH} < 10$  cm are trees that died after 2010. Low Decay: decay class 1; Moderate Decay: decay classes 2 or 3; Advanced Decay: decay classes 4 or 5. **Fig. S8.** Snag dynamics for *Pinus lambertiana* (sugar pine) in the Yosemite Forest Dynamics Plot from 2011 to 2018. Snag persistence and fall rates were calculated as changes in the snag population between summer field seasons. The vertical dotted line represents the fire event in the fall of 2013. Because snags  $1 \leq \text{DBH} < 10$  cm were not included in the dataset at plot establishment, all snags  $1 \leq \text{DBH} < 10$  cm are trees that died after 2010. Low Decay: decay class 1; Moderate Decay: decay classes 2 or 3; Advanced Decay: decay classes 4 or 5. **Fig. S9.** Snag dynamics for *Pinus lambertiana* in the Yosemite Forest Dynamics Plot from 2011 to 2018 by density, basal area, and volume. The vertical dotted line represents the fire event in the fall of 2013. Because snags  $1 \leq \text{DBH} < 10$  cm were not included in the dataset at plot establishment, all snags  $1 \leq \text{DBH} < 10$  cm are trees that died after 2010. Low Decay: decay class 1; Moderate Decay: decay classes 2 or 3; Advanced Decay: decay classes 4 or 5. **Fig. S10.** Snag dynamics for *Quercus kelloggii* (California black oak) in the Yosemite Forest Dynamics Plot from 2011 to 2018. Snag persistence and fall rates were calculated as changes in the snag population between summer field seasons. The vertical dotted line represents the fire event in the fall of 2013. Because snags  $1 \leq \text{DBH} < 10$  cm were not included in the dataset at plot establishment, all snags  $1 \leq \text{DBH} < 10$  cm are trees that died after 2010. Low Decay: decay class 1; Moderate Decay: decay classes 2 or 3; Advanced Decay: decay classes 4 or 5. **Fig. S11.** Snag dynamics for *Quercus kelloggii* in the Yosemite Forest Dynamics Plot from 2011 to 2018 by density, basal area, volume, and carbon (C) content. The vertical dotted line represents the fire event in the fall of 2013. Because snags  $1 \leq \text{DBH} < 10$  cm were not included in the dataset at plot establishment, all snags  $1 \leq \text{DBH} < 10$  cm are trees that died after 2010. Low Decay: decay class 1; Moderate Decay: decay classes 2 or 3; Advanced Decay: decay classes 4 or 5. **Table S6.** All predictor variables initially considered for modeling snag fall. Diameter class thresholds based on crown injury represent the 0–20<sup>th</sup> percentile (least scorched; 1–9 cm DBH), 20–40<sup>th</sup> percentile (10–14 cm DBH), 40–60<sup>th</sup> percentile (15–20 cm DBH), 60–80<sup>th</sup> percentile (20–27 cm DBH), and >80<sup>th</sup> percentile ( $\geq 28$  cm DBH). Diameter class thresholds for snags were  $1 \leq \text{DBH} < 10$  cm,  $10 \leq \text{DBH} < 60$  cm, and  $\text{DBH} \geq 60$  cm DBH. Pre-fire Neighborhood and Neighborhood Fire Severity metrics were calculated within annuli of radii 0–3, 3–6, 6–9, 9–12, and 12–15 m surrounding each focal snag. <sup>a</sup>Variable only applied to snags in the post-fire populations. **Table S7.** Model inputs for four selected models. Bold, italicized blue text indicates variables that were confirmed by Boruta, were retained after collinear variables were removed, and were run as inputs to random forest. Bold text indicates variables that were confirmed by Boruta but were removed because they exceeded the collinearity threshold for that model and were not selected to be kept. Numbers in parentheses are mean importance values averaged across 15 runs of random forest. Variables in bold, italicized blue text are ordered by mean importance value. **Fig. S12.** Random forest model accuracy metrics for models of the fall of pre-fire snags  $\text{DBH} \geq 10$  cm. Model accuracy was determined by 10-fold cross validation. Panel rows indicate whether the models were constrained to pre-fire or post-fire predictor variables. Within each panel, seven models occupy seven rows (see Manuscript Table 2);

the accuracy of each model is represented by the three boxplots that occupy that row. The boxplots represent the distribution of the model accuracy of 15 random forest analyses, each run with a different seed. The *r*-values indicate the maximum level of collinearity between predictor variables. **Fig. S13.** Random forest metrics for models of the fall of post-fire snags  $\text{DBH} \geq 10$  cm. Model accuracy was determined by 10-fold cross validation. Panel rows indicate whether the models were constrained to pre-fire or post-fire predictor variables. Within each panel, models occupy six or seven rows (see Manuscript Table 2); the accuracy of each model is represented by the three boxplots that occupy that row. The boxplots represent the distribution of the model accuracy of 15 random forest analyses, each run with a different seed. The *r*-values indicate the maximum level of collinearity between predictor variables. **Fig. S14.** Random forest metrics for models of the fall of post-fire snags  $\text{DBH} \geq 10$  cm run with balanced data. To verify whether an imbalance in snag outcomes was driving the difference in sensitivity and specificity for the post-fire snag population, which is slightly imbalanced, we randomly selected subsets of the more common outcome to generate a balanced dataset: 2,315 snags were randomly selected without replacement from the 5,907 snags that persisted. Five random draws were run on each of three seeds. When we reran the random forest models with balanced data, the results resembled the pre-fire snag population models: sensitivity tended to be the higher metric and, for each model, the difference between sensitivity and specificity was reduced. Model accuracy was determined by 10-fold cross validation. Panel rows indicate whether the models were constrained to pre-fire or post-fire predictor variables. Within each panel, models occupy six or seven rows (see Manuscript Table 2); the accuracy of each model is represented by the three boxplots that occupy that row. The boxplots represent the distribution of the model accuracy of those 15 random forest analyses. The *r*-values indicate the maximum level of collinearity between predictor variables. **Fig. S15.** Correlation matrix of important continuous variables in the most predictive model (i.e., 0–3 m neighborhood,  $r = 0.7$ ) that used just post-fire variables to predict fall of pre-fire snags  $\text{DBH} \geq 10$  cm (See Manuscript Table 2). Variables that correlated with at least one other variable at  $r^2 > |0.15|$  were selected for display. See SI Table 6 for predictor variable definitions. **Fig. S16.** Correlation matrix of important continuous variables in the most predictive model (i.e., 0–15 m neighborhood,  $r = 0.7$ ) that used just pre-fire variables to predict fall of pre-fire snags  $\text{DBH} \geq 10$  cm (See Manuscript Table 2). See SI Table 6 for predictor variable definitions. **Fig. S17.** Correlation matrix of important continuous variables in the most predictive model that used the most predictive model that used just post-fire variables (i.e., 0–6 m neighborhood,  $r = 0.7$ ) to predict fall of post-fire snags  $\text{DBH} \geq 10$  cm (See Manuscript Table 2). See SI Table 6 for predictor variable definitions. **Fig. S18.** Correlation matrix of important continuous variables in the most predictive model (i.e., 0–3 m neighborhood,  $r = 0.5$ ) that used just pre-fire variables to predict fall of post-fire snags  $\text{DBH} \geq 10$  cm (See Manuscript Table 2). See SI Table 6 for predictor variable definitions. **Fig. S19.** Partial dependence plots of the nine most important continuous pre-fire predictor variables in random forest models of the fall of pre-fire snags  $\text{DBH} \geq 10$  cm. Solid lines represent mean partial dependence values from 15 model runs. Gray dotted lines represent minimum and maximum partial dependence values from the 15 model runs. Density units are trees  $\text{ha}^{-1}$ . Basal area units are  $\text{m}^2 \text{ha}^{-1}$ . Volume units are  $\text{m}^3 \text{ha}^{-1}$ . **Fig. S20.** Partial dependence plots of the nine most important continuous post-fire predictor variables in random forest models of the fall of pre-fire snags  $\text{DBH} \geq 10$  cm. Vertical red dashed lines and the corresponding values indicate thresholds that were used to categorize snags in multi-variate partial dependence plots (Manuscript Fig. 4). Solid lines represent mean partial dependence values from 15 model runs. Gray dotted lines represent minimum and maximum partial dependence values from the 15 model runs. Density units are trees  $\text{ha}^{-1}$ . Basal area units are  $\text{m}^2 \text{ha}^{-1}$ . Biomass units are  $\text{Mg ha}^{-1}$ . **Fig. S22.** Partial dependence plots of the nine most

important continuous post-fire predictor variables in random forest models of the fall of post-fire snags DBH  $\geq 10$  cm. Solid lines represent mean partial dependence values from 15 model runs. Gray dotted lines represent minimum and maximum partial dependence values from the 15 model runs. Basal area units are  $\text{m}^2 \text{ha}^{-1}$ .

### Acknowledgements

The Yosemite Forest Dynamics Plot is a collaborative project of Utah State University, the University of Montana, and Washington State University. We thank Yosemite National Park for providing logistical support and the students, volunteers, and staff individually listed at <http://yfdp.org> for data collection. Thank you to Joseph Birch for measuring the movement of coarse woody debris. Thank you to Martin Holdrege, Susan Durham, Erika Blomdahl, Justin DeRose, Sara Germain, Tucker Furniss, Sean Jeronimo, Janneke HilleRisLambers, Andrew Kulmatiski, Nate Stephenson, Larissa Yocom, and two anonymous reviewers for comments that improved the manuscript.

### Authors' contributions

K.M.L.B. assisted with the data collection, analyzed the data, and wrote the manuscript. J.A.L. assisted with the data collection and supervised the manuscript preparation.

### Funding

Funding for this research was provided by a National Science Foundation Graduate Research Fellowship under Grant Number DGE-1745048; the Smithsonian ForestGEO; the Joint Fire Science Program (award 16-1-04-02), the National Park Service (awards P14AC00122 and P14AC00197); the Ecology Center at Utah State University; the University of Montana Wilderness Institute; and the Utah Agricultural Experiment Station (projects 1153 and 1398), which has designated this as journal paper number 9557.

### Availability of data and materials

The data used in this study can be obtained by filling out a data request form through the Smithsonian ForestGEO data portal (<https://forestgeo.si.edu>).

### Declarations

#### Ethics approval and consent to participate

Not applicable.

#### Consent for publication

Not applicable.

#### Competing interests

The authors declare that they have no competing interests.

#### Author details

<sup>1</sup>Wildland Resources Department, Utah State University, 5230 Old Main Hill, Logan, UT 84322-5230, USA. <sup>2</sup>The Ecology Center, Utah State University, 5230 Old Main Hill, Logan, UT 84322-5230, USA.

Received: 27 October 2022 Accepted: 9 October 2023

Published online: 23 November 2023

### References

- Allen, C.D., A.K. Macalady, H. Chenchouni, et al. 2010. A global overview of drought and heat-induced tree mortality reveals emerging climate change risks for forests. *Forest Ecology and Management* 259: 660–684. <https://doi.org/10.1016/j.foreco.2009.09.001>.
- Bagne, K.E., K.L. Purcell, and J.T. Rotenberry. 2008. Prescribed fire, snag population dynamics, and avian nest site selection. *Forest Ecology and Management* 255: 99–105. <https://doi.org/10.1016/j.foreco.2007.08.024>.
- Barth, M.A.F., A.J. Larson, and J.A. Lutz. 2015. A forest reconstruction model to assess changes to Sierra Nevada mixed-conifer forest during the fire suppression era. *Forest Ecology and Management* 354: 104–118. <https://doi.org/10.1016/j.foreco.2015.06.030>.
- Battles JJ, Cousins SJM, Sanders JE (2015) Carbon dynamics and greenhouse gas emissions of standing dead trees in California mixed conifer forests. Berkeley, California, USA.
- Biging, G.S. 1984. Taper equations for second-growth mixed conifers of Northern California. *Forest Science* 30: 1103–1117.
- Blomdahl, E.M., C.A. Kolden, A.J.H. Meddens, and J.A. Lutz. 2019. The importance of small fire refugia in the central Sierra Nevada, California, USA. *Forest Ecology and Management* 432: 1041–1052. <https://doi.org/10.1016/j.foreco.2018.10.038>.
- Bull, E.L., and T.W. Heater. 2000. Resting and denning sites of American martens in Northeastern Oregon. *Northwest Science* 74: 179–185 <http://hdl.handle.net/2376/1018>.
- Butts, S.R., and W.C. McComb. 2000. Associations of forest-floor vertebrates with coarse woody debris in managed forests of western Oregon. *The Journal of Wildlife Management* 64: 95–104.
- Campbell, J., D. Donato, D. Azuma, and B. Law. 2007. Pyrogenic carbon emission from a large wildfire in Oregon, United States. *Journal of Geophysical Research* 112: 1–11.
- Cansler, C.A., M.E. Swanson, T.J. Furniss, et al. 2019. Fuel dynamics after reintroduced fire in an old-growth Sierra Nevada mixed-conifer forest. *Fire Ecology* 15: 1–17. <https://doi.org/10.1186/s42408-019-0035-y>.
- Chambers, C.L., and J.N. Mast. 2005. Ponderosa pine snag dynamics and cavity excavation following wildfire in northern Arizona. *Forest Ecology and Management* 216: 227–240. <https://doi.org/10.1016/j.foreco.2005.05.033>.
- Conner, R.N., D. Saenz, R.N. Conner, and D. Saenz. 2005. The longevity of large pine snags in eastern Texas. *Wildlife Society Bulletin* 33: 700–705.
- Cousins, S.J.M., J.J. Battles, J.E. Sanders, and R.A. York. 2015. Decay patterns and carbon density of standing dead trees in California mixed conifer forests. *Forest Ecology and Management* 353: 136–147. <https://doi.org/10.1016/j.foreco.2015.05.030>.
- Cutler, R.D., T.H. Edwards, K.H. Beard, et al. 2007. Random forests for classification in ecology. *Ecology* 88: 2783–2792. <https://doi.org/10.1890/07-0539.1>.
- Dahms W (1949) How long do ponderosa pine snags stand? Portland, OR.
- Das, A.J., N.L. Stephenson, and K.P. Davis. 2016. Why do trees die? Characterizing the drivers of background tree mortality. *Ecology* 97: 2616–2627. <https://doi.org/10.1002/ecy.1497>.
- Davies SJ, Abiem I, Abu Salim K, et al (2021) ForestGEO: understanding forest diversity and dynamics through a global observatory network. *Biological Conservation* 253: <https://doi.org/10.1016/j.biocon.2020.108907>.
- Dunn, C.J., and J.D. Bailey. 2012. Temporal dynamics and decay of coarse wood in early seral habitats of dry-mixed conifer forests in Oregon's Eastern Cascades. *Forest Ecology and Management* 276: 71–81. <https://doi.org/10.1016/j.foreco.2012.03.013>.
- Everett, R., J. Lehmkuhl, R. Schellhaas, et al. 1999. Snag dynamics in a chronosequence of 26 wildfires on the east slope of the Cascade Range in Washington state, USA. *International Journal of Wildland Fire* 9: 223–234. <https://doi.org/10.1071/wf00011>.
- Franklin, J.F., D. Lindenmayer, J.A. MacMahon, et al. 2000. Threads of continuity. *Conservation Biology in Practice* 1: 8–16. <https://doi.org/10.1111/j.1526-4629.2000.tb00155.x>.
- Furniss TJ, Larson AJ, Kane VR, Lutz JA (2020) Wildfire and drought moderate the spatial elements of tree mortality. *Ecosphere* 11: <https://doi.org/10.1002/ecs2.3214>.
- Gabrielson, A.T., A.J. Larson, J.A. Lutz, and J.J. Reardon. 2012. Biomass and burning characteristics of sugar pine cones. *Fire Ecology* 8: 58–70. <https://doi.org/10.4996/fireecology.0803058>.
- Gaines, E.M., H.R. Kallander, and J.A. Wagner. 1958. Controlled burning in southwestern ponderosa pine: results from the Blue Mountain Plots, Fort Apache Indian Reservation. *Journal of Forestry* 56: 323–327.
- Ganey, J.L., J.M. Iniguez, S.C. Vojta, and A.R. Iniguez. 2021. Twenty years of drought-mediated change in snag populations in mixed-conifer and ponderosa pine forests in Northern Arizona. *Forest Ecosystems* 8: 1–13.
- Garber, S.M., J.P. Brown, D.S. Wilson, et al. 2005. Snag longevity under alternative silvicultural regimes in mixed-species forests of central Maine. *Canadian Journal of Forest Research* 35: 787–796. <https://doi.org/10.1139/x05-021>.
- Goodwin, M.J., H.S.J. Zald, M.P. North, and M.D. Hurteau. 2021. Climate-driven tree mortality and fuel aridity increase wildfire's potential heat flux. *Geophysical Research Letters* 48: 1–6. <https://doi.org/10.1029/2021GL094954>.
- Grayson, L.M., D.R. Cluck, and S.M. Hood. 2019. Persistence of fire-killed conifer snags in California, USA. *Fire Ecol* 15: 1–14. <https://doi.org/10.1186/s42408-018-0007-7>.



- Greenwell, B. 2018. *pdp: partial dependence plots*. CRAN Repos. version 0.7.0.
- Harmon, M.E., J.F. Franklin, F.J. Swanson, et al. 1986. Ecology of coarse woody debris in temperate ecosystems. *Adv Ecol Res* 15: 133–302.
- Harmon ME, Woodall CW, Fasth B, Sexton J (2008) Woody detritus density and density reduction factors for tree species in the United States: a synthesis. USDA Gen Tech Rep NRS-29 USDA For Serv North Res Stn 84.
- Hijmans, R.J. 2020. *Raster: geographic data analysis and modeling*. CRAN Repos. version 3, 3–13.
- Innes, J.C., M.P. North, and N. Williamson. 2006. Effect of thinning and prescribed fire restoration treatments on woody debris and snag dynamics in a Sierran old-growth, mixed-conifer forest. *Canadian Journal of Forest Research* 36: 3183–3193. <https://doi.org/10.1139/X06-184>.
- Jeronimo, S.M.A., J.A. Lutz, R. Kane V, et al. 2020. Burn weather and three-dimensional fuel structure determine post-fire tree mortality. *Landscape Ecology* 35: 859–878. <https://doi.org/10.1007/s10980-020-00983-0>.
- Keen, F.P. 1929. How soon do yellow pine snags fall? *Journal of Forestry* 27: 735–737.
- Knapp, E.E. 2015. Long-term dead wood changes in a Sierra Nevada mixed conifer forest: Habitat and fire hazard implications. *Forest Ecology and Management* 339: 87–95. <https://doi.org/10.1016/j.foreco.2014.12.008>.
- Kursa MB, Rudnicki WR (2010) Feature selection with the boruta package. *Journal of Statistical Software* 36:1–13. <https://doi.org/10.18637/jss.v036.i11>.
- Kursa MB, Rudnicki WR (2020) *Boruta: wrapper algorithm for all relevant feature selection*. CRAN Repos. version 7.00 1–17.
- Liaw, A., and M. Wiener. 2018. *Briemain and Cutler's random forests for classification and regression*. version 4.6-14.
- Lutz, J.A. 2015. The evolution of long-term data for forestry: large temperate research plots in an era of global change. *Ozone: Science & Engineering* 89: 255–269. <https://doi.org/10.3955/046.089.0306>.
- Lutz, J.A., A.J. Larson, M.E. Swanson, and J.A. Freund. 2012. Ecological importance of large-diameter trees in a temperate mixed-conifer forest. *PLoS One* 7: e36131. <https://doi.org/10.1371/journal.pone.0036131>.
- Lutz, J.A., K.A. Schwindt, T.J. Furniss, et al. 2014. Community composition and allometry of *Leucothoe davisiae*, *Cornus sericea*, and *Chrysolepis sempervirens* *Canadian Journal of Forest Research* 44: 1–7. <https://doi.org/10.1139/cjfr-2013-0524>.
- Lutz, J.A., T.J. Furniss, S.J. Germain, et al. 2017. Shrub communities, spatial patterns, and shrub-mediated tree mortality following reintroduced fire in Yosemite National Park, California, USA. *Fire Ecology* 13: 104–126. <https://doi.org/10.4996/fireecology.1301ppp>.
- Lutz, J.A., J.R. Matchett, L.W. Tarnay, et al. 2017. Fire and the distribution and uncertainty of carbon sequestered as aboveground tree biomass in Yosemite and Sequoia & Kings Canyon National Parks. *Land* 6: 1–24. <https://doi.org/10.3390/land6010010>.
- Lutz, J.A., T.J. Furniss, D.J. Johnson, et al. 2018. Global importance of large-diameter trees. *Global Ecology and Biogeography* 27: 849–864. <https://doi.org/10.1111/geb.12747>.
- Lutz, J.A., S. Struckman, T.J. Furniss, et al. 2020. Large-diameter trees dominate snag and surface biomass following reintroduced fire. *Ecological Processes* 9: 1–13. <https://doi.org/10.1186/s13717-020-00243-8>.
- Lutz, J.A., S. Struckman, T.J. Furniss, et al. 2021. Large-diameter trees, snags, and deadwood in southern Utah, USA. *Ecological Processes* 10: 1–12. <https://doi.org/10.1186/s13717-020-00275-0>.
- Lyon, L.J. 1977. *Attrition of lodgepole pine snags on the Sleeping Child Burn, Montana*. Ogden.
- van Mantgem, P.J., N.L. Stephenson, J.C. Byrne, et al. 2009. Widespread increase of tree mortality rates in the western United States. *Science (80- )* 323: 521–524. <https://doi.org/10.1126/science.1165000>.
- Maser, C., and J. Trappe. 1984. *The seen and unseen world of the fallen tree*.
- Meyer, M.D., D.A. Kelt, and M.P. North. 2005. Nest trees of Northern flying squirrels in the Sierra Nevada. *Journal of Mammalogy* 86: 275–280. <https://doi.org/10.1644/BEH-110.1>.
- Michel, L.A., D.J. Peppe, J.A. Lutz, et al. 2014. Remnants of an ancient forest provide ecological context for Early Miocene fossil apes. *Nature Communications* 5: 1–9. <https://doi.org/10.1038/ncomms4236>.
- Mitchell, R.G., and H.K. Preisler. 1998. Fall rate of lodgepole pine killed by the mountain pine beetle in Central Oregon. *Western Journal of Applied Forestry* 13: 23–26. <https://doi.org/10.1093/wjaf/13.1.23>.
- Monsanto, P.G., and J.K. Agee. 2008. Long-term post-wildfire dynamics of coarse woody debris after salvage logging and implications for soil heating in dry forests of the eastern Cascades, Washington. *Forest Ecology and Management* 255: 3952–3961. <https://doi.org/10.1016/j.foreco.2008.03.048>.
- Morrison, M.L., and M.G. Raphael. 1993. Modeling the dynamics of snags. *Ecological Applications* 3: 322–330.
- Parks, S.A., and J.T. Abatzoglou. 2020. Warmer and drier fire seasons contribute to increases in area burned at high severity in western US forests from 1985 to 2017. *Geophysical Research Letters* 47: 1–10. <https://doi.org/10.1029/2020GL089858>.
- PRISM Climate Group. 2016. *PRISM 800-m climate normals (1981-2010)*.
- R Core Team. 2020. *R: a language and environment for statistical computing*.
- Rabe, M.J., T.E. Morrell, H. Green, et al. 1998. Characteristics of ponderosa pine snag roosts used by reproductive bats in northern Arizona. *The Journal of Wildlife Management* 62: 612–621. <https://doi.org/10.2307/3802337>.
- Raphael, M.G., and M. White. 1984. Use of snags by cavity-nesting birds in the Sierra Nevada. *Wildlife Monographs* 86: 3–66.
- Ritchie, M.W., E.E. Knapp, and C.N. Skinner. 2013. Snag longevity and surface fuel accumulation following post-fire logging in a ponderosa pine dominated forest. *Forest Ecology and Management* 287: 113–122. <https://doi.org/10.1016/j.foreco.2012.09.001>.
- Runkle, J.R. 2013. Thirty-two years of change in an old-growth Ohio beech-maple forest. *Ecology* 94: 1165–1175. <https://doi.org/10.1890/11-2199.1>.
- Russell, R.E., V. a Saab, J.G. Dudley, and J.J. Rotella. 2006. Snag longevity in relation to wildfire and postfire salvage logging. *Forest Ecology and Management* 232: 179–187. <https://doi.org/10.1016/j.foreco.2006.05.068>.
- Russell, M.B., and a R. Weiskittel. 2012. Assessing and modeling snag survival and decay dynamics for the primary species in the Acadian forest of Maine, USA. *Forest Ecology and Management* 284: 230–240. <https://doi.org/10.1016/j.foreco.2012.08.004>.
- Scholl, A.E., and A.H. Taylor. 2010. Fire regimes, forest change, and self-organization in an old-growth mixed-conifer forest, Yosemite National Park, USA. *Ecological Applications* 20: 362–380. <https://doi.org/10.1890/08-2324.1>.
- Stavros, N.E., Z. Tane, V.R. Kane, et al. 2016. Unprecedented remote sensing data over King and Rim megafires in the Sierra Nevada Mountains of California. *Ecology* 97: 3334. <https://doi.org/10.1002/ecy.1577>.
- Stephens, S.L., B.M. Collins, C.J. Fettig, et al. 2018. Drought, tree mortality, and wildfire in forests adapted to frequent fire. *BioScience* 68: 77–88. <https://doi.org/10.1093/biosci/bix146>.
- Stephens, S.L., A.A. Bernal, B.M. Collins, et al. 2022. Mass fire behavior created by extensive tree mortality and high tree density not predicted by operational fire behavior models in the southern Sierra Nevada. *Forest Ecology and Management* 518: 1–12. <https://doi.org/10.1016/j.foreco.2022.120258>.
- Thomas, J.W. 1979. *Wildlife habitats in managed forests: the Blue Mountains of Oregon and Washington*. Washington: D.C., USA.
- Thomas, S.C., and A.R. Martin. 2012. Carbon content of tree tissues: a synthesis. *Forests* 3: 332–352. <https://doi.org/10.3390/f3020332>.
- Ucitel, D., D.P. Christian, and J.M. Graham. 2003. Vole use of coarse woody debris and implications for habitat and fuel management. *Journal of Wildlife Management* 67: 65–72.
- van Wagtenonk, J.W., and J.A. Lutz. 2007. Fire regime attributes of wildland fires in Yosemite National Park, USA. *Fire Ecology* 3: 34–52. <https://doi.org/10.4996/fireecology.0302034>.
- van Wagtenonk, J.W., P.E. Moore, J.L. Yee, and J.A. Lutz. 2020. The distribution of woody species in relation to climate and fire in Yosemite National Park, California, USA. *Fire Ecology* 16: 1–23. <https://doi.org/10.1186/s42408-020-00079-9>.
- Varner, J.M., S.M. Hood, D.P. Aubrey, et al. 2021. Tree crown injury from wildland fires: causes, measurement and ecological and physiological consequences. *The New Phytologist* 231: 1676–1685. <https://doi.org/10.1111/nph.17539>.
- Wensel, L.C., and B. Krumland. 1983. *Volume and taper relationships for redwood, Douglas fir, and other conifers in California's north coast*. Division of Agricultural Sciences Bulletin 1907, University of California.
- Wensel, L.C., and C.M. Olson. 1995. Tree taper model volume equations. *Hilgardia* 62: 67.
- Zeibig-Kichas, N.E., C.W. Ardis, J.-P. Berrill, and J.P. King. 2016. Bark thickness equations for mixed-conifer forest type in Klamath and Sierra Nevada Mountains of California. *International Journal of Forestry Research* 2016: 1–10. <https://doi.org/10.1155/2016/1864039>.

## Publisher's Note

Springer Nature remains neutral with regard to jurisdictional claims in published maps and institutional affiliations.